EFDA–JET–CP(13)01/11

K. Heinola, C.F. Ayres, A. Baron-Wiechec, J.P. Coad, J. Likonen, G.F. Matthews,
A. Widdowson and JET EFDA contributors

Tile Profiler Analysis of Samples from JET ITER-Like Wall and Carbon Wall

Tile Profiler Analysis of Samples from JET ITER-Like Wall and Carbon Wall

K. Heinola[1,2], C.F. Ayres[1], A. Baron-Wiechec[1], J.P. Coad[1], J. Likonen[3], G.F. Matthews[1], A. Widdowson[1] and JET EFDA contributors*

JET-EFDA, Culham Science Centre, OX14 3DB, Abingdon, UK

[1]EURATOM-CCFE Fusion Association, Culham Science Centre, OX14 3DB, Abingdon, OXON, UK
[2]Association EURATOM-TEKES, University of Helsinki, PO Box 64, 00560 Helsinki, Finland
[3]Association EURATOM-TEKES, VTT, PO Box 1000, 02044, VTT, Espoo, Finland
** See annex of F. Romanelli et al, "Overview of JET Results", (24th IAEA Fusion Energy Conference, San Diego, USA (2012)).*

Preprint of Paper to be submitted for publication in Proceedings of the 14th International Conference on Plasma-Facing Materials and Components for Fusion Applications, Jülich, Germany.
13th May 2013 - 17th May 2013

ABSTRACT

A complete global balance for material transport in JET requires knowledge of the net erosion in the main chamber, net deposition in the divertor and the amount of dust in the divertor region. Following the end of the first JET ITER-Like Wall campaign a set of tiles has been removed from the main chamber and the divertor. This paper describes the initial tile surface profiling results for evaluating the erosion in the main chamber and deposition in the divertor. Tile profiling was performed on upper dump plate tiles, inner wall guard limiters made of beryllium and on inner divertor tiles made of tungsten coated carbon-fibre composites. Additionally, the mass of dust collected from the JET divertor is also reported. Present results are compared with JET-C campaign results with the all carbon wall.

1. INTRODUCTION

In 2010 the JET plasma-facing wall was converted from all-carbon (C) wall to metallic wall. The new wall configuration comprises of beryllium (Be) in the main chamber and tungsten (W) on the divertor region and is known as ITER-Like Wall (ILW). The ILW is designed to demonstrate the differences in material transport and hydrogen isotope retention compared to all-C wall and to help predict the behaviours of ITER in these respects. In detail, the transition from all-C JET-C wall to metallic JET-ILW composed of changing from graphite and carbon fibre composite (CFC) tile elements to bulk Be, Be coated inconel or W coated CFC tiles in the main chamber and W coated CFC with one row of bulk W in the divertor. The first JET-ILW campaign 2011-2012 was followed with an intervention where set of tiles from main chamber and divertor were removed from the vessel for surface analyses. A priori tile removal the divertor region was vacuumed for collecting any dust formed during JETILW operation. The post-mortem analyses of plasma-facing tiles and dust form the fundamental basis for understanding the erosion and deposition of wall material and material migration patterns inside the vessel during JET operation.

In this paper mass of Be eroded from the main chamber is evaluated and compared to the deposition and dust found on the W divertor. Results from first JET-ILW campaign 2011-2012 with metal wall are compared with JET-C campaign 2007–2009 all-C wall results.

2. EXPERIMENTAL

The erosion and deposition of the inner wall guard limiters (IWGL) and the dump plate tiles from the main chamber and tiles from the divertor was measured by profiling a set of tiles before and after exposure in the vessel. Moreover, a high-resolution in-vessel imaging survey was carried out before tiles were being taken off the vessel wall. Once were received from the vessel, a detailed photographic surface study was performed for each tile. Tiles for profiling comprised of upper and midplane IWGL tiles, upper dump plates and inner divertor tiles 1, 3 and 4. Figure 1 shows the poloidal locations of the investigated tiles.

The profiler consists of a X–Y table and a Z probe. The tile to be profiled is mounted onto the

X-Y table, which is then moved using two stepper motors according to a pre-determined series of (X,Y) coordinates thus forming a measurement grid. At each grid point the Z probe is extended to touch the surface of the tile. The relative value for the height is recorded for each grid point and as a result a cloud of measurement points is obtained. These points correspond to the tile surface. The grid step used in X and Y direction is 5mm.

By comparing the grid measurements on a tile before and after exposure in the JET vessel, changes of the tile surface topography can be obtained, and assessment of erosion and deposition of tile surface can be made. Repeatability measurements provide profiler accuracy in Z direction within few microns, however, the major source of measurement error arises from the positioning of the tile. Presently, measurement of a single tile is considered accepted when three sequential profiling measurement results – including re-positioning of the tile – are statistically 5μm of each other.

Based on profiler results the volume of the eroded and deposited material can be determined. A density of $\rho_{Be} = 1.85 g/cm^2$ has been used for both erosion of bulk Be tiles and for deposition on W coated divertor tiles for converting the profiled volume to deposited mass. The chosen ρBe is approximation for the present JET-ILW results – it is probable that identical densities can not be used for describing bulk Be erosion and deposition. The deposition measured with surface profiling may be found in different forms with co-deposited impurities (such as carbon, oxygen and deuterium) on tiles removed from different locations of the vessel; Be thin films can be formed on W and/or Be can be mixed with W leading to Be-W mixing or even alloying. Presently, the character of deposited layers are being studied further with Ion Beam Analysis (IBA) methods [3].

By assuming toroidal symmetry, the obtained mass of eroded/deposited Be is scaled with the number of similar tiles found in the vessel to give global net erosion/deposition. Figure 1 shows the tiles used in the present study for estimating net values. Moreover, Be erosion and deposition rates are determined by dividing the obtained erosion/deposition mass by the plasma exposure time. Erosion and deposition rates (γ^{ero} and γ^{depo}) have been calculated for limiter plasma configuration times and for total plasma times, respectively. It is assumed that Be erosion takes place only during the limiter phase plasma configuration only. Excluding X-point plasma phase from the calculations and using only limiter plasma time allows making direct correlation with the measured erosion profiles from the limiter tiles. Total plasma time for JET-ILW and JET-C was 19h and 45h, of which limiter phase was 6h and 12h.

Loose dust was collected using a vacuum cleaner and cyclone adapted for use by remote handling. A cyclone pot was installed at the bottom of the cyclone to capture dust sample during vacuuming. Two different vacuum samples were collected from the divertor into cyclone pots. Regions for collection were; the outer divertor (Load Bearing Tile and tiles 6, 7, 8, B and C) and the inner divertor (High Field Gap Closure tile and tiles 1, 3 and 4). JET-ILW vacuuming was not extended to cover the louvre areas. Cyclone pots were weighed before and after vacuuming for determining the mass of dust collected. The vacuuming samples covered 92% (330º out of 360º) of the whole

vessel divertor area, the remaining two out of 24 divertor modules were reserved for post mortem analyses and the corresponding module tiles were preserved. Presented dust results are scaled to represent 24 modules.

3. RESULTS

3.1 UPPER DUMP PLATES

Visual inspection of the removed upper dump plate tiles (identification of tiles 2B(C)1, 2B(C)2, 2B(C)3, 2B(C)4 and 2B(C)5) showed two main characteristic surface features. All of the dump plates had surface melting and molten material migration in the centre part of the tile, i.e. the ridge region, whereas tracks due to arcing were observed only on one side of the tile (Fig.2). Although the melting and arc tracks varied from tile to tile poloidally, the high-resolution in-vessel imaging survey confirmed toroidal symmetry of these surface features.

The dump plate ridge region is closest to and has highest interaction with the plasma. Surface with arc tracks can be found on tile side facing directly the plasma current (Fig.2). The melt surface damage extends from the ridge region to the other side without arc tracks. The melt material migration was found to be upwards filling and bridging neighbouring castellations on the tile. This upwards motion is due to the j×B forces and coincides with reported IWGL melt layer motion of JET-ILW [7]. However, metallic droplets were observed on the divertor tiles and it is highly plausible that these droplets are originating from the melting events of Be dump plates. The characterisation of these droplets is taking place 2013–2014. It is likely, that the melting events are due to disruptions and took place before active use of Disruption Mitigation Valve system [6]. Even though the melting events were extending throughout the tile surface, the amplitude of the damage varied locally considerably and was found to be far less than the profiler grid density. The determination of the erosion of upper dump plates is under investigation.

3.2 INNER WALL GUARD LIMITER

Erosion and deposition of JET-ILW IWGL tiles from the horizontal mid-plane (identification 2XR10) and from the upper end (identification 2XR19) of the limiter beam (indicated in Fig.1) have been evaluated by the surface profiling. Visual inspection results of IWGLs are summarized in [9]. Both upper and mid-plane tiles showed high surface roughness on the right wing (Fig.3). This roughness is likely due to changes in tile surface morphology caused by high heat and particle load from the plasma. The solid and rough surface region resembles re-solidified molten surface. The far end of left wing showed marks due to arcing on both the upper and the mid-plane IWGL tiles.

Upper IWGL tile showed deposition profile with thickness of ~5μm on the right-hand side of the centre area, i.e. the ridge region. On the left side of the ridge the profiling resulted in erosion of <2μm. Taking into account the accuracy of 5μm of the Z probe it can be concluded, that erosion and deposition in the upper IWGL is in the limits of the present surface profiler accuracy and no absolute conclusions can be drawn.

Mid-plane IWGL showed strong erosion in the ridge region and throughout the centre area of the tile (Fig.3). Using value $\rho_{Be} = 1.85 g/cm^2$ yields to 0.8g of Be gross erosion for one mid-plane IWGL tile assuming all of the erosion takes place during the limiter plasma configuration. It is worth to mention, that the heat flux measurements on IWGLs [1] have shown a temperature profile extending poloidally to the neighbouring tiles of the mid-plane tile. However, in present work the erosion from poloidally neighbouring tiles has not been assessed and the erosion result is given for mid-plane IWGL tile only. Taking into account the JETILW limiter phase time of 6 hrs yields for erosion rate $\gamma_{Be}^{ero} = 3.7 \times 10^{-4}$ g/s per midplane tile. In the vessel are ten mid-plane IWGL tiles positioned toroidally, which yields 8.0g and $\gamma_{Be,\,tot}^{ero} = 3.7 \times 10^{-4}$ g/s for total Be gross erosion and erosion rate in the vessel during limiter phase, respectively. Taking into account the fact that no clear erosion was observed in the upper IWGL, it can be speculated that mid-plane region of IWGLs act as a high Be erosion source. However, it is assumed that the eroded Be from the IWGL gets locally deposited and does not get transported to the divertor region. Further investigations on other tiles in the vessel, such as inner wall cladding tiles, will take place for identifying other Be sources.

For JET-C 2007-2009 it has been previously shown that mid-plane IWGL did act as the main C erosion source [10]. Figure 4 shows surface profiling result for one C IWGL mid-plane tile. It is important to note, that the shown profiling result is from tile that has been exposed in the vessel from 2005 to 2009. In the following all the C tile calculations are done by scaling the gross erosion result presented in Fig.4 from 2005–2009 to cover period 2007–2009. Using C density of $\rho_C = 1.65 g/cm^3$ results in C gross erosion 0.8g for one C IWGL mid-plane tile during limiter phase of 12h (out of total plasma time 45h). The obtained gross erosion yields for C erosion rate $\gamma_C^{ero} = 1.9 \times 10^{-5}$ g/s per tile for the limiter phase. Comparison with the JET-ILW erosion rate leads to the conclusion that during limiter phase the Be erosion rate is higher than C erosion rate per one mid-plane IWGL tile with a ratio of $\gamma_{Be}^{ero} : \gamma_C^{ero} = 1.95 : 1$. The higher erosion rate of Be tile might be due to high physical sputtering and efficient self-sputtering of Be at inner limiter shown in earlier experiments in JET [8, 2]. It is worth to keep in mind the global erosion during JET-C being larger since in JET-C there were sixteen C IWGLs installed in the vessel. It leads to 12.8g and $\gamma_{C,\,tot}^{ero} = 3.0 \times 10^{-4}$ g/s for total C gross erosion and erosion rate for all the C mid-plane IWGL tiles in the vessel during limiter phase, respectively.

3.3 INNER DIVERTOR

Surface profiler results have been evaluated for JET-ILW inner divertor tiles 1, 3 and 4 and results are shown in Fig.5. Most of the deposition was found on the upper part of tile 1 and additional deposition was found on tile 3. The toroidal net deposition on tile 1 and on tile 3 was found to be 19.5g and 15.3g, respectively. Deposition on tile 1 is expected to be higher than the obtained profiling result, since the profiler grid did not extend to the apron of tile 1. According to the IBA results for tile 1, there is large amount of deposition found on the apron region [3]. For this reason, the profiler result for tile 1 needs to considered as a minimum value for deposition. The erosion/

deposition profile along tile 4 was ±2μm which is less than the profiler accuracy. Combining profiling results for tile 1, 3 and 4 leads to inner divertor net deposition of >34.8g during JET-ILW campaign. Result is a factor of ten less than C net deposition obtained from the JET-C 2007-2009 campaign for inner divertor >312g [9].

The net deposition rates for inner divertor is calculated by taking into account the total plasma exposure times during JET-ILW and JET-C 2007-2009. It is assumed that the observed net deposition takes place during both the limiter and the X-point plasma configuration. Based on this it can be concluded that the inner divertor net deposition rate for JET-ILW yields $\gamma^{depo}_{Be,\,net} = 5.1\times10^{-4}$g/s and for JET-C $\gamma^{depo}_{C,\,net} = 1.9\times10^{-3}$ g/s. The ratio of these rates is $\gamma^{depo}_{Be,\,net} : \gamma^{depo}_{C,\,net} = 1 : 3.73$. Difference in deposition rates favouring JET-C might be due to larger areal C source in the machine and charge exchange neutrals causing chemical erosion in the C main chamber. The Be erosion source for the JET-ILW inner divertor deposition is currently under investigation. There is no evident connection with the IWGL limiter phase Be erosion and the net deposition found on the inner divertor. It is assumed that the eroded Be particles get locally deposited on IWGLs and do not get ransported to the divertor region. This would indicate the inner divertor deposition taking place during the X-point configur ation, but the Be source needs to be verified with further surface analyses and e.g. with spectroscopic measurements of the plasma.

There is a notable difference in the locations of the deposited areas in the inner divertor for JET-ILW and JET-C. Both campaigns have shown deposition on tile 1, but the striking difference is in the lack of deposition on tile 4 in JET-ILW, whereas in JET-C the vast majority of deposition was found on tile 4. This is a direct correlation with the locations of the strike points during the campaigns. In Fig.5 is shown time which the inner strike point was located on different tiles during JET-ILW campaign (Pulse No's: 79854 – 83794) and JET-C campaign (Pulse No's: 70959 – 79836). In JET-ILW the inner strike point was most of the campaign on tile 3, whereas in JET-C it was on tile 4. However, during JET-C strike point time on tile 3 was same as with JET-ILW, which was seen as deposition in JET-C [10]. In addition during JET-ILW the strike point was on tile 4, but there was no deposition observed with surface profiling.

3.4 DIVERTOR DUST

Dust collected from the inner and outer divertor after the JET-ILW campaign and JET-C 2007-2009 campaign are summarised in Fig.6. The total amount of dust collected is ~1g and ~180g for JET-ILW and JET-C, respectively. It is probable that most of the JET-ILW dust was located in the divertor region during start-up discharges of the campaign. Moreover, in JET-C the dust formation had reached an equi librium. For C deposits the critical thickness is 120μm, above which the the deposit does not get any thicker but spalls and converts to dust. Exposure time of C tiles has been long enough in JET-C for reaching this critical thickness providing continuous dust formation. Analysing the composition of the JET-ILW divertor dust will take place in 2013 – 2014.

CONCLUSIONS

First surface profiling data for determining erosion and deposition of JET-ILW main chamber and divertor tiles are presented. Analysis was performed on upper and mid-plane IWGL tiles, inner divertor tiles and upper dump plate tiles. Results show the mid-plane IWGL tile being Be erosion dominated area. Dump plate region may act as an additional Be erosion source via melting events, but this was not confirmed with tile profiling. Inner divertor deposition was seen on tile 1 and on location of the inner strike point on tile 3.

Tentative results for limiter phase show an erosion rate of 3.7×10^{-5} g/s for Be IWGL mid-plane tile, whereas a lower erosion rate of 1.9×10^{-5}g/s was obtained for C IWGL mid-plane tile. Assuming toroidal symmetry yields a global gross erosion of 6.4g and 12.8g for JET-ILW and JET-C IWGL mid-plane tiles, correspondingly. This difference is due to the larger number of IWGL beams installed; JET-ILW has ten IWGLs whereas JET-C was installed with sixteen IWGLs. These erosion results are highly preliminary and it is unlikely that only mid-plane IWGL tile is acting as an erosion source. Further analyses including spectroscopic results of heat flux distribution on IWGL and Be impurity emission lines are needed in assessing the contribution of other poloidal IWGL tiles to the gross erosion. Hence, the presented IWGL erosion results represent the minimum erosion.

The preliminary result for toroidal net deposition on inner divertor for JETILW and JET-C was >35g and >312g, respectively. The order of magnitude difference in net depositions might be explained with larger C source in the machine and partially with larger erosion yield during X-point plasma configuration.

Presented results are preliminary and further studies are needed for understaning the global erosion and deposition balance of JET-ILW. Tiles from the lower IWGL, outer divertor and outer poloidal limiter will be surface analysed during 2013–2014. In addition, the composition of ILW deposited layers is turning out to be an important study subject. Depending on whether deposited layer is composed of Be thin film, Be-W mixed layer and/or has formed an Be-W alloy, these different composition types may show different deposition properties which will have an effect in determining the global net deposition. Experimental and computational studies on densities and structural properties of deposited layers of exposed JET-ILW tiles are taking place 2013–2014.

ACKNOWLEDGEMENTS

This work, part-funded by the European Communities under the contract of Association EURATOM/CCFE and Association EURATOM-TEKES was carried out within the framework of the European Fusion Development Agreement. The views and opinions expressed herein do not necessarily reflect those of the European Commission.

REFERENCES

[1]. G. Arnoux, et al., I-14, 14th International Conference on Plasma-facing Materials and Components for Fusion Applications, Aachen, Germany (2013)

[2]. D. Borodin, M.F. Stamp, A. Kirschner, C. Björkas, S. Brezinsek, et al., Journal of Nuclear Materials, in press (2013), http://dx.doi.org/10.1016/j.jnucmat.2013.01.043
[3]. P. Coad, et al., C-17, 14th International Conference on Plasmafacing Materials and Components for Fusion Applications, Aachen, Germany (2013)
[4]. K. Krieger, S. Brezinsek, M. Reinelt, S.W. Lisgo, J.W. Coen en, et al., Journal of Nuclear Materials, in press (2013), http://dx.doi.org/10.1016/j.jnucmat.2013.01.042
[5]. G. F. Matthews, Journal of Nuclear Materials, in press (2013), http://dx.doi.org/10.1016/j.jnucmat.2013.01.282
[6]. C. Reux, M. Lehnen, U. Kruezi, S. Jachmich, P. Card, et al., Fusion Engineering and Design, in press (2013), http://dx.doi.org/10.1016/j.fusengdes.2012.12.026
[8]. G. Sergienko, et al., A-104, 14th International Conference on Plasma-facing Materials and Components for Fusion Applications, Aachen, Germany (2013)
[8]. M. Stamp, K. Krieger, S. Brezinsek, JET-EFDA contributors, Journal of Nuclear Materials **415**, S170 (2011)
[9]. A. Widdowson, et al., I-15, 14th International Conference on Plasma-facing Materials and Components for Fusion Applications, Aachen, Germany (2013)
[10]. A. Widdowson, C.F. Ayres, S. Booth, J.P. Coad, A. Hakola, et al., Journal of Nuclear Materials, in press (2013), http://dx.doi.org/10.1016/j.jnucmat.2013.01.179

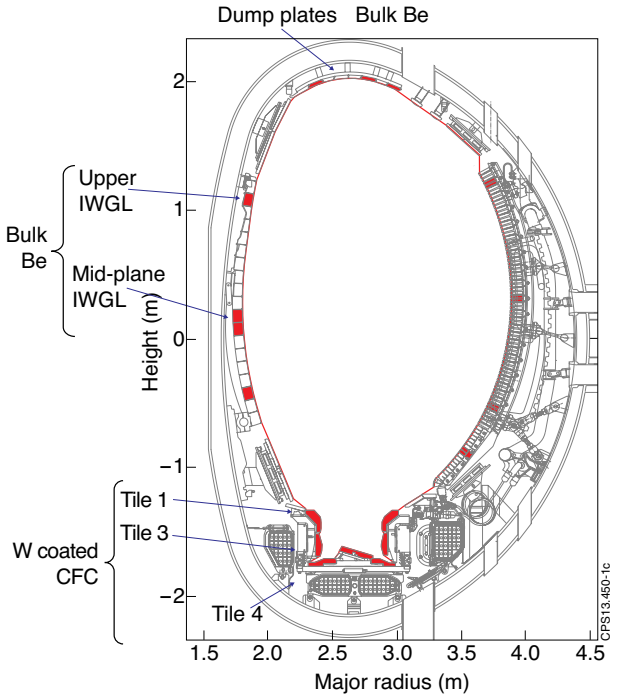

Figure 1: Poloidal cross section of JET vessel. The tiles with results presented in this paper are indicated.

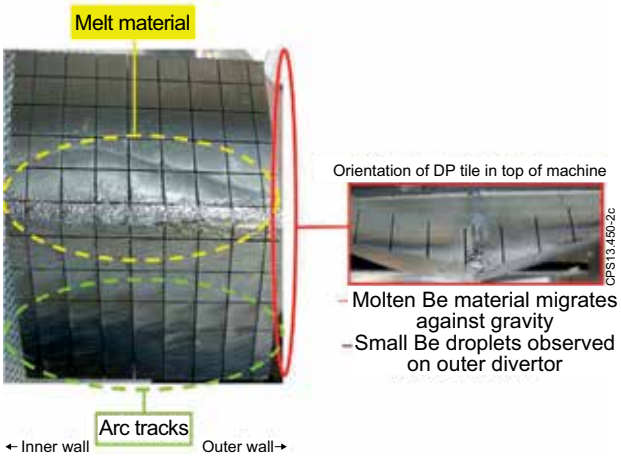

Figure 2: Observed surface features on JET-ILW dump plate tiles. Each tile shows patterns of melting on the ridge area and tracks due to arcing on plasma current side of tile. Amount of surface damage varies poloidally but is symmetric toroidally. Melt Be material motion proceeds upwards, but small Be droplets were observed on divertor tiles.

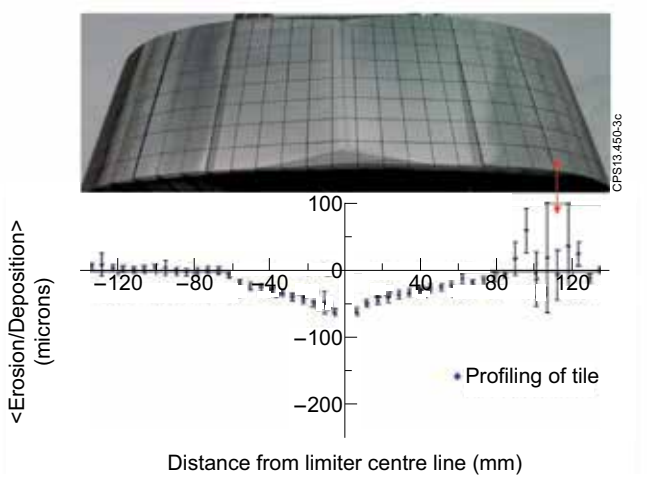

Figure 3: Surface profiling result for JET-ILW mid-plane IWGL tile. Main Be erosion zone is in the centre of tile. Calculated tile gross erosion is 0.8g and tile erosion rate 3.7×10^{-5} g/s (see text for details). The red arrow indicates area with high surface roughness due to surface morphology changes after plasma interacting with the tile.

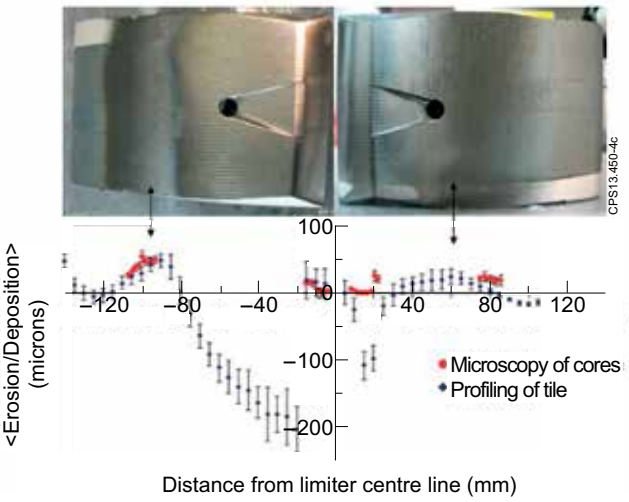

Figure 4: Surface profiling result for JET-C Wall mid-plane IWGL tile [Widdowson13a]. Main C erosion source is in the middle of the tile. Compensating erosion to JET-C campaign period 2007-2009 yields to a tile gross erosion of 0.8g with a tile erosion rate of 1.9×10^{-5} g/s (see text for details). The arrows indicate areas with highest deposition.

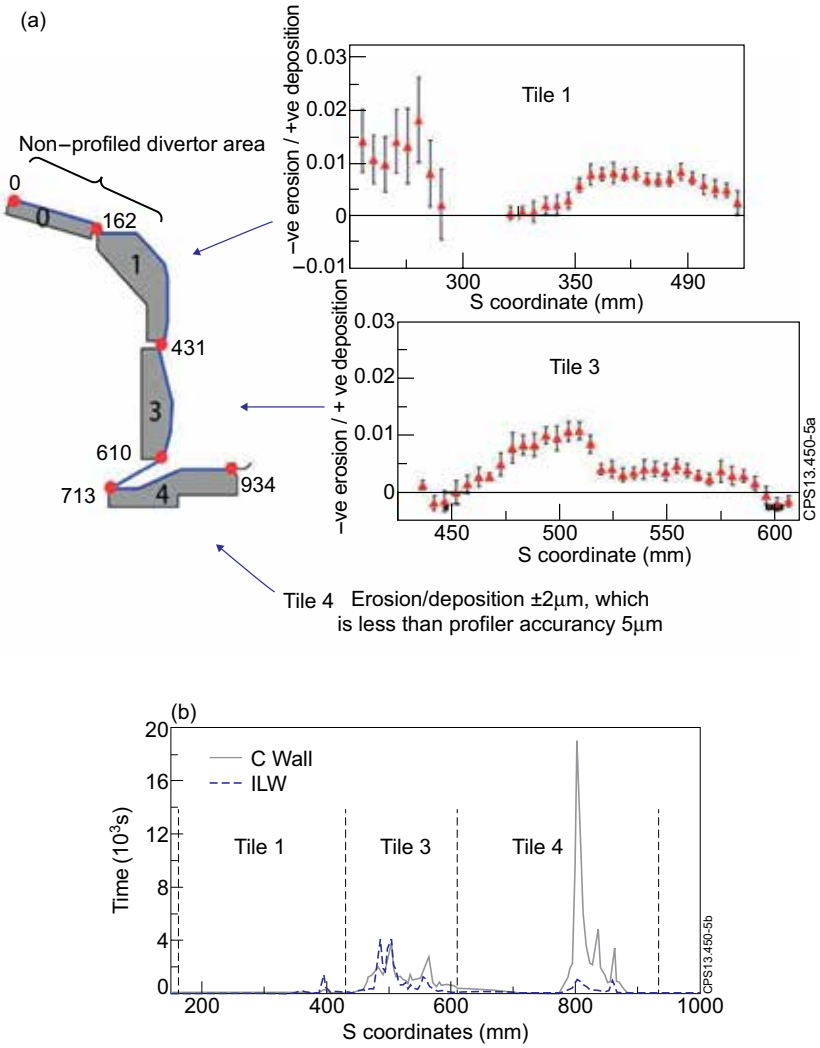

Figure 5: a) Profiler results for JET-ILW inner divertor tiles 1, 3 and 4. The S coordinates show the locations of profiled sections. Area not being covered by surface profiling is highlighted in the figure. b) Inner strike point time exposure time on different tiles during JET-ILW and JET-C. The JET-ILW tile 3 deposition and lack of deposition on tile 4 may be related to strike point locations during the campaign. During JET-C campaign most of deposition on inner divertor was measured on tile 4, which correlates with the strike point time [10].

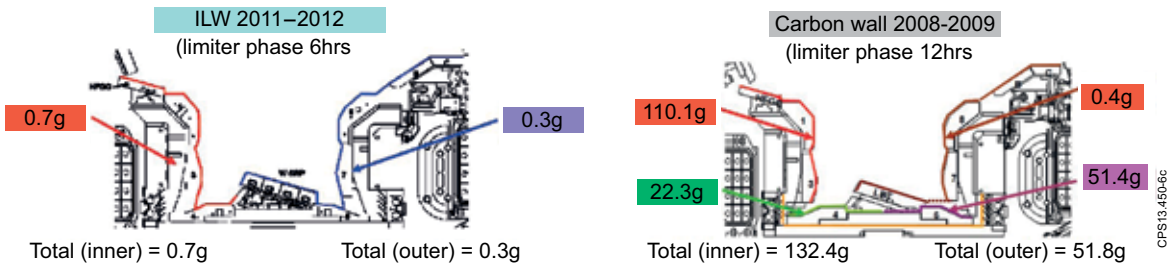

Figure 6: Amount of dust collected after the JET-ILW campaign (left) and JET-C campaign (right). Dust results are scaled with shown limiter phase plasma time [10].